2023 5th International Conference on Telecommunication and Photonics (ICTP)
December 21-23, Dhaka, Bangladesh

On the Performance of Intelligent Reflecting Surface Aided Industrial Internet of Things Networks

Neelanjana Subin Ferdous*, Md Sahabul Alam†, M. Shifatul Islam‡, Lutfa Akter§,
Kamrul Hasan¶ and Imtiaz Ahmed**
*Department of Electrical and Electronic Engineering, Bangladesh University, Dhaka, Bangladesh.
†Department of Electrical and Computer Engineering, California State University, Northridge, CA, USA.
‡,§Department of Electrical and Electronic Engineering, Bangladesh University of Engineering and Technology, Dhaka, Bangladesh.
¶Department of Electrical and Computer Engineering, Tennessee State University, Nashville, TN, USA.
**Department of Electrical Engineering and Computer Science, Howard University, Washington DC, USA.
Email: neelanjanaeece6@gmail.com, md-sahabul.alam@csun.edu

2023 IEEE International Conference on Telecommunications and Photonics (ICTP) | 979-8-3503-9347-7/23/$31.00 ©2023 IEEE | DOI: 10.1109/ICTP60248.2023.10490628

***Abstract*—This paper considers an Industrial Internet of Things (IIoT) environment and explores the utilizations of Intelligent Reflecting Surface (IRS) panels to improve the reliability of data transmissions. The effect of boundary walls and reflected signals in an indoor IIoT setting are accounted for in the analysis. Two multi-IRS-aided schemes are considered, that is, Exhaustive IRS-aided (ERA) scheme and Opportunistic IRS-aided (ORA) scheme, and their performances are evaluated by analyzing the outage probabilities (OPs). Extensive simulation studies underscore the significant improvements in wireless communication performance and reliability brought about by deploying IRS panels in IIoT environments.**

***Index Terms*—Intelligent Reflecting Surface (IRS), Industrial Internet of Things (IIoT), Outage Probability (OP), Cumulative Distribution Function (CDF).**

I. Introduction

With the evolution of fifth-generation (5G) and beyond, wireless networks and Industrial Internet of Things (IIoT) have enhanced the efficiency and performance of a smart industry by improving connectivity between humans and machines in an industrial setting. Thus, industrial wireless communication or IIoT is a key driving factor for improving manufacturing and industrial processes. However, industrial wireless communications face more difficulties than traditional wireless communications because of metallic structures, electromagnetic interference, randomly moving objects (such as robots and vehicles), room size, or thick building structures [1]. On the other hand, complete industrial automation demands ultra-reliability and low-latency communications (URLLC) in order to deliver sensor data and actuation instructions at precise instants with specified reliability. These challenges even become more critical with the collaboration of humans and machines in Industry 5.0. Moreover, the increasing demand for a variety of novel services in smart factories like holographic control display systems, augmented reality (AR) / virtual reality (VR) maintenance, etc. will introduce new communication challenges to industrial networks [2]. To satisfy the communication requirements of such services, IIoT entails some advanced technologies. Intelligent Reflecting Surface (IRS) is one of such state-of-the-art and emerging technologies.

IRS consists of an array of small and low-cost passive reflecting elements that can adjust the phase and amplitude of the incident signals [3]. Furthermore, in a challenging scenario where the direct line of sight (LOS) link between transceivers is severely blocked, as is common in the industrial environment due to heavy and movable machinery, IRS can produce a virtual LOS link to bypass the hindrance between transceivers via smart reflection [4]. Moreover, IRS allows the enhancement of signal quality by creating extra signal links between transceivers. Compared to a single IRS, multiple IRSs provide additional benefits [5], [6]. Thus, by strategically placing multiple IRSs in an IIoT environment, it is possible to achieve even more significant improvements, i.e., more coverage and capacity, reduced interference, and increased energy efficiency. Additionally, using multiple IRSs allows for more flexible and dynamic control of the wireless communication environment, enabling the efficient use of available resources and the ability to adapt to changing conditions.

Despite being a promising scenario, there has been little research done on the use of multiple IRSs. For instance, in [7], the advantages of multiple IRSs assisted wireless systems were investigated by analyzing the error performance for both outdoor and indoor scenarios. In the case of a multi-IRS scenario, as IRSs are placed in random locations, even if one or two IRSs suffer from deep fading, communication can still be established by other IRSs to the destination. These links can be combined with direct link to enhance the received power at the receiver. Consequently, it is vital to analyze the performance of such systems that comprise the direct link with multiple IRSs reflected paths to access the increased power at the receiver [8], [9]. In [8], two schemes were proposed for a multi-IRS-aided wireless system; exhaustive IRS-aided (ERA) scheme and opportunistic IRS-aided (ORA) scheme. In ERA, all of the available IRSs help to establish links between the source and the destination whereas in ORA, only the IRS that provides the best signal-to-noise ratio (SNR) is considered. The performances of the proposed IRS architectures were analyzed by deriving tight approximate closed-form expressions for the outage probability (OP) and ergodic capacity (EC). Further-

more, to evaluate the performance of a multi-IRS system, a closed-form expression of the symbol error probability (SEP) was derived considering Nakagami-m fading channels in [9]. Authors in [10] designed a joint active and passive precoding to maximize the received signal power using multiple IRSs in mm-wave communications. Considering a device-to-device (D2D) URLLC transmission, a joint optimization design of active and passive beamforming is formulated in [11] to maximize the number of actuators with successful decoding. In [12], a path-loss model for indoor factories is derived, and the performance of the proposed model is evaluated in terms of the effective capacity for URLLC service considering cm- and mm-wave bands. Recently, [13]–[15] demonstrated the potential of cooperative passive beamforming and beam routing, considering inter-IRS reflections. In particular, [13] developed a joint active/passive beamforming algorithm for scenarios lacking direct base station (BS)-user links. Extending this work, [14], [15] formulated a cascaded LOS link between a BS and a remote user, and designed optimal IRS selection and beam routing methods for maximizing the cascaded channel power gain.

However, the majority of the existing IRS research primarily focuses on outdoor applications, with a limited exploration into IIoT in factories. In this paper, we focus on an indoor IIoT setting with multiple IRS panels aiding data transmission for transceivers. We consider both ERA and ORA IRS-panel participation schemes and analyze the OP performances of both schemes. Unlike outdoor environments, the impact of boundary walls and the signals reflected from the boundary walls are taken into account along with the direct link for the considered multi-IRS system.

The rest of this paper is organized as follows. The system and signal models are described in Section II. Section III explores the ERA and ORA IRS-panel participation schemes considering the impact of reflected signals. Numerical results and discussions are provided in Section IV, where the impacts of the system parameters are evaluated in detail. Finally, Section V concludes the paper.

II. System Model

We consider an indoor IIoT environment that spans an area of $50 \times 50\text{m}^2$. Assuming the transmitter and receiver are positioned at an identical height, we depict the IIoT model within a two-dimensional (2D) framework represented as $\mathcal{I}$, where the walls are situated along both the X and Y axes. Therefore, a signal transmitted from the source S is subject to multipath propagation, reflecting off the walls to reach the destination D. Note that both S and D can be positioned anywhere within the area designed as $\mathcal{I}$. We consider the direct and the R reflected propagation paths for the analysis as shown in Fig. 1. Associated direct and reflected path distances between the source and receiver are calculated using simple geometry.

We consider N IRS panels are scattered randomly in $\mathcal{I}$, where each IRS consists of L_n elements, where $n \in \{1, 2, \cdots, N\}$. Let us define the small-scale channel fading for

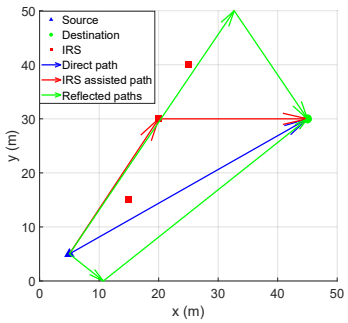

Fig. 1: System model for an indoor environment composed of an S, a D, and IRS panels (assuming, N=3 and R=2).

the direct path and reflected path $r \in \{1, 2, \dots R\}$, between S and D as complex random variables $h_{SD} = |h_{SD}|e^{j\theta_0}$ and $h^r_{SD} = |h^r_{SD}|e^{j\theta^r_0}$, respectively. Here, $|\cdot|$ represents the absolute value of a complex variable. In particular, $|h_{SD}|$ is modeled as Nakagami-m fading with shape parameter m_0 and spread parameter Ω_0 [16]. Likewise, $|h^r_{SD}|$ follows Nakagami-m distributions with shape and spread parameters represented as m_r and Ω_r, respectively. Note that θ_0 and θ^r_0 present the random phases following uniform distributions (between 0 and 2π) associated with the direct path and reflected path R, respectively.

Furthermore, we define the small-scale channel gain between S and the passive reflecting element (PRE) $l \in \{1, 2, \cdots, L_n\}$ of IRS $n \in \{1, 2, \cdots, N\}$ as $h_{nl} = |h_{nl}|e^{j\phi_{nl}}$. Likewise, the channel gain between PRE l of IRS n and D is represented as $g_{nl} = |g_{nl}|e^{j\psi_{nl}}$. Both $|h_{nl}|$ and $|g_{nl}|$ are assumed to follow Nakagami-m distributions. In particular, the shape parameters for the channels between the source to IRS and IRS to destination are defined as m_{hn} and m_{gn}, respectively, whereas the spread parameters are denoted as Ω_{hn} and Ω_{gn}, respectively for $n \in \{1, 2, \cdots, N\}$. The phases associated with IRS-panels ϕ_{nl} and ψ_{nl} follow uniform distributions that randomly change between 0 and 2π. The amplification factor of PRE $l \in \{1, 2, \cdots, L_n\}$ for IRS $n \in \{1, 2, \cdots, N\}$ is defined as κ_{nl}, and the phase associated with the element is termed as Θ_{nl}.

S transmits signal x_S with power $P_S = \mathbb{E}\{|x_S|^2\}$, where $\mathbb{E}$ denotes statistical expectation. The signal received at D is corrupted by additive white Gaussian noise (AWGN) w_D having zero mean and variance σ^2_D. We consider 3GPP Urban Micro model to calculate path loss (in log-scale) $PL(\text{dB}) = -22.7 - 26 \times \log_{10} f_c - 36.7 \times \log_{10} d$. Here, f_c and d represent the carrier frequency and transmission distance, respectively.

III. IRS-Participation Protocols

In this paper, we examine two IRS-participation protocols, namely ERA and ORA, to illustrate the role of IRS panels in aiding communication between S and D.

A. The exhaustive IRS-aided (ERA) protocol

In this protocol, the phases of the PREs in each of N IRS-panels are tuned optimally to provide optimal performance. The signal received at D for the considered protocol can be expressed as:

TABLE I: The Simulation Setup.

Parameters	Values
Source coordinate	(5,5)
Destination coordinate	(45,30)
Number of IRS panels, N	5
IRS coordinates	(15,15), (20, 30), (25,40) (30, 5), (35,25)
Number of elements in IRS, L_n	$\{25, 36, 49\}$
Direct path distance, d_{SD} (m)	47.16
Number of reflected paths, R	2
Reflected path distance, d^r_{SD}(m)	53.14, 76.31
Nakagami shape parameters	$U[2, 3]$
Nakagami spread parameters	2
Simulation times	10^4
Spectral efficiency threshold, R_{th} (bits/s/Hz)	1
Carrier frequency, fc (GHz)	3
Signal bandwidth (MHz)	10
Noise power (dB)	-174
Gain of the source (dB)	5
Gain of the IRS elements (dB)	5
Gain of the receiver (dB)	0

$$y^{\text{ERA}} = \sqrt{P_S}\big(h_{SD}e^{j\theta_0} + \sum_{r=1}^{R} h^r_{SD}e^{j\theta^r_0} + \sum_{n=1}^{N}\sum_{l=1}^{Ln} h_{nl}e^{j\phi_{nl}}g_{nl}e^{j\psi_{nl}}\kappa_{nl}e^{j\Theta_{nl}}\big)x_S + w_D. \quad (1)$$

The first term of y^{ERA} in (1) emerges from the effect of the direct path transmission, whereas the second term contains the impact of all the reflected paths. The third term of y^{ERA} in (1) yields the effect of IRS-assisted paths. Defining the phase error $\delta_{nl} = \Theta_{nl} + \phi_{nl} + \psi_{nl} - \theta_0$, (1) can be stated as follows:

$$y^{\text{ERA}} = \sqrt{P_S}e^{j\theta_0}\Big(h_{SD} + \sum_{r=1}^{R} h^r_{SD}e^{j(\theta^r_0-\theta_0)} + \sum_{n=1}^{N}\sum_{l=1}^{Ln} h_{nl}g_{nl}\kappa_{nl}e^{j\delta_{nl}}\Big)x_s + w_D.$$

In order to provide constructive interference at D and thereby assure optimal data transmissions, we need to satisfy $\delta_{nl} = 0$, $\forall n$, $\forall l$. As such, the phases of PREs in the active IRS-panels will yield $\Theta^*_{nl} = \theta_0 - (\phi_{nl} + \psi_{nl})$. Applying Θ^*_{nl} and $\left|e^{j\theta_0}\right|^2 = 1$, y^{ERA} can be defined as follows:

$$y^{\text{ERA}} = \sqrt{P_S}e^{j\theta_0}\Big(h_{SD} + \sum_{r=1}^{R} h^r_{SD}e^{j(\theta^r_0-\theta_0)} + \sum_{n=1}^{N}\sum_{l=1}^{Ln} h_{nl}g_{nl}\kappa_{nl}\Big)x_s + w_D \quad (2)$$

Let us denote the received signal-to-noise ratio (SNR) as γ_{ERA}, which can be calculated from (2) and represented as follows:

$$\gamma^{\text{ERA}} = \rho\left|h_{SD} + \sum_{r=1}^{R} h^r_{SD}e^{j(\theta^r_0-\theta_0)} + \sum_{n=1}^{N}\sum_{l=1}^{Ln} h_{nl}g_{nl}\kappa_{nl}\right|^2, \quad (3)$$

where $\rho = P_S/\sigma^2_D$. Note that γ_{ERA} is leveraged to analyze the performances of the considered scheme by calculating the cumulative distribution function (CDF) and OP.

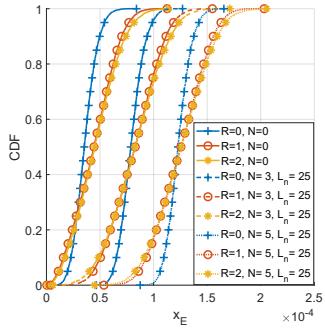

(a) CDF for the distributions

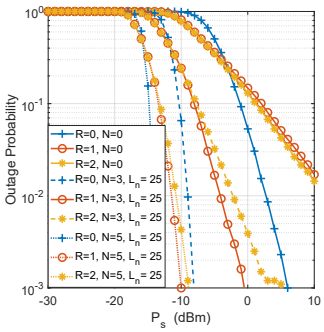

(b) OP as a function of P_S

Fig. 2: Performance of the ERA Scheme for different numbers of N and R.

B. The opportunistic IRS-aided (ORA) protocol

For ORA protocol, the best IRS-panel is selected to participate in data transmission. This protocol offers an energy-efficient and simpler receiver design because of low computational complexity. The signal received at D via IRS-panel n (for ORA) can be expressed as follows:

$$y^{\text{ORA}} = \sqrt{P_S}e^{j\theta_0}\Big(h_{SD} + \sum_{r=1}^{R} h^r_{SD}e^{j(\theta^r_0-\theta_0)} + \sum_{l=1}^{Ln} h_{nl}g_{nl}\kappa_{nl}\Big)x_S + w_D. \quad (4)$$

Moreover, γ^{ORA}_n can be presented as

$$\gamma^{\text{ORA}}_n = \rho\left|h_{SD} + \sum_{r=1}^{R} h^r_{SD}e^{j(\theta^r_0-\theta_0)} + \sum_{l=1}^{Ln} h_{nl}g_{nl}\kappa_{nl}\right|^2. \quad (5)$$

Let us denote the index of the best IRS-panel as $\tilde{n} \in \{1, 2, \cdots, N\}$, which provides the maximum received SNR $\gamma^{\text{ORA}}_{\tilde{n}}$ among all the active IRS-panels, where $\Theta^*_{\tilde{n}l} = \theta_0 - (\phi_{\tilde{n}l} + \psi_{\tilde{n}l})$. Note that $\tilde{n}$ is calculated by applying the best-IRS panel selection metric as follows:

$$\tilde{n} = \arg\max_{1\le\hat{n}\le N} \gamma^{\text{ORA}}_{\hat{n}}. \quad (6)$$

IV. Performance Evaluation

Let us define random variables $x_E = \sqrt{(\gamma^{\text{ERA}}/\rho)}$ and $x_O = \sqrt{(\gamma^{\text{ORA}}/\rho)}$ and evaluate their CDFs. A Monte Carlo simulation is performed over the distribution of each random variables described in Section II. From the CDF we proceed

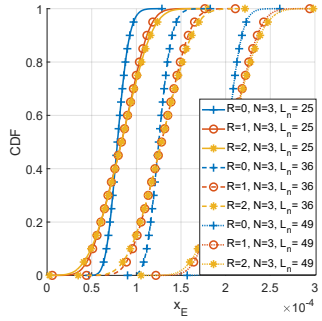

(a) CDF for the distributions

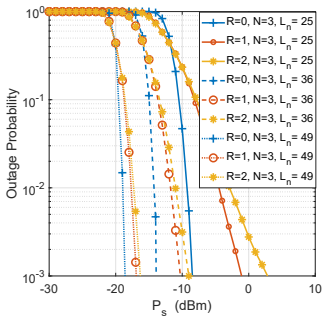

(b) OP as a function of P_S

Fig. 3: Performance of the ERA Scheme for different numbers L_n and R.

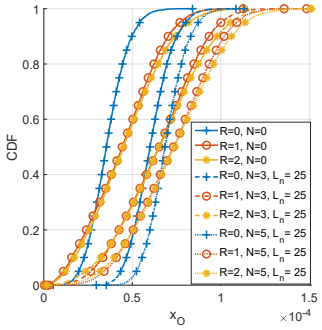

(a) CDF for the distributions

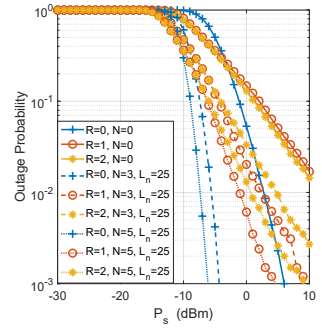

(b) OP as a function of P_S

Fig. 4: Performance of the ORA scheme with different numbers of N and R.

to compute the OP for both IRS aided systems. The OP is defined as the probability that the mutual information at any instance is below a certain defined spectral efficiency threshold R_{th}.

For the Monte Carlo simulation, 10^4 number of instances have been averged to get the specific results. In our setup, R is varied from 0 (which corresponds to the outdoor environment) to 2 respectively. N is varied from 0 (which corresponds to no IRS) to 5. L_n in each IRS is varied to observe the effect on transmission characteristics. The geometric configuration of the system model and the simulation parameters are presented in Table I.

A. Performance of ERA scheme

Fig. 2 shows the CDF and OP of the ERA scheme with the different numbers of N. From Fig. 2a we observe that the CDF of the received signal shifts towards higher values of x_E with increasing the number of N. This shift is linear with the increasing number of N. It is also observed that the addition of the reflected paths increases the spread of the distribution while keeping the mean of the distribution in roughly the same location. The CDF function translates into the OP in Fig. 2b. From this figure, we observe that the OP decreases with the inclusion of N, and the improvement is linear with N. Also, the higher variance in the CDF results in a reduction of OP with the addition of reflected paths. This observation suggests that in the indoor environment, the ERA scheme will perform slightly worse than in the outdoor environment, where there are no reflected paths to corrupt the direct signal. Fig. 3 describes the performance of the ERA scheme with an increasing number of L_n. From the CDF in Fig. 3a we observe that the distribution shifts towards higher values with increasing the number of L_n. The corresponding OPs are presented in Fig. 3b, where the ERA scheme's performance improves with the increasing number of L_n. Also, as in the previous case, adding the number of reflected paths increases the variance of the distributions, thereby degrading the performance of the transmission.

B. Performance of ORA scheme

Fig. 4 shows the performance of the ORA scheme with varying numbers of N. From the CDF distributions we again observe that with increasing the number of N, the CDF shift towards higher values (See Fig. 4a), which translates into better performance in terms of OP (See Fig. 4b). However, unlike the ERA scheme, the improvement is not linear with the number of N, instead reaches out to a saturation level. Furthermore, the addition of reflected paths increases the spread of the signals, thereby degrading the outage probability of the system.

Fig. 5 illustrates the performance of the opportunistic IRS scheme with varying L_n and the presence of reflected paths. As expected, the increasing number of L_n shifts the CDF linearly towards the right (see Fig. 5a), thereby improving the outage performance (see Fig. 5b). This improvement is linear with the increasing number of L_n.

C. Comparing between ERA and ORA Schemes

Comparing Eqs. (2) with (4) we can further understand the characteristics of the performance improvement offered by both the ERA and ORA-assisted schemes. First of all, in the

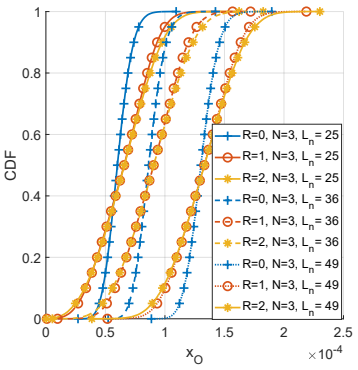

(a) CDF for the distributions

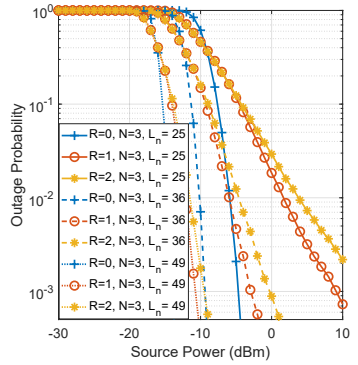

(b) OP as a function of P_S

Fig. 5: Performance of the ORA scheme with different numbers of L_n and R.

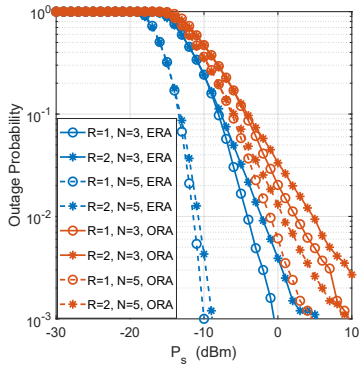

Fig. 6: OP comparison between ERA and ORA.

ERA scheme, the N number of IRS panels with L_n number of elements per IRS: all contribute to the IRS-assisted link, whereas in the opportunistic scheme, only the L_n elements from the optimal IRS choice contribute to the performance enhancement. Therefore we would expect the ERA scheme to perform better than the ORA scheme. Comparing the OPs between these two schemes (see Fig. 6) agrees to this expectation, and it shows that the ERA scheme performs better than the ORA scheme even after the signal quality is degraded in the presence of several reflected paths in the indoor environment. However, the ORA scheme yields a diversity order identical to ERA while assuring less computational complexity because of reduced signaling overhead.

V. Conclusions

This work emphasized the significance of IRS panels to improve the reliability of data transmissions in an indoor IIoT environment. Two IRS-assisted schemes are considered, namely: Exhaustive IRS-aided scheme (ERA) and opportunistic IRS-aided scheme (ORA). We evaluated the outage performances of both schemes considering the impact of reflected signals from the boundary walls. Simulation results positively affirm that both ERA and ORA schemes exhibit certain performance constraints due to strong (indoor) signal reflections, rendering the IRS-aided mechanisms relatively less efficient for indoor settings compared to outdoor environments.

References

[1] F. Firyaguna, J. John, M. O. Khyam, D. Pesch, E. Armstrong, H. Claussen, H. V. Poor *et al.*, "Towards industry 5.0: Intelligent reflecting surface (IRS) in smart manufacturing," *arXiv preprint arXiv:2201.02214*, 2022.

[2] K. B. Letaief, W. Chen, Y. Shi, J. Zhang, and Y.-J. A. Zhang, "The roadmap to 6g: Ai empowered wireless networks," *IEEE communications magazine*, vol. 57, no. 8, pp. 84–90, 2019.

[3] Q. Wu, S. Zhang, B. Zheng, C. You, and R. Zhang, "Intelligent reflecting surface-aided wireless communications: A tutorial," *IEEE Transactions on Communications*, vol. 69, no. 5, pp. 3313–3351, 2021.

[4] S. Gong, X. Lu, D. T. Hoang, D. Niyato, L. Shu, D. I. Kim, and Y.-C. Liang, "Toward smart wireless communications via intelligent reflecting surfaces: A contemporary survey," *IEEE Communications Surveys & Tutorials*, vol. 22, no. 4, pp. 2283–2314, 2020.

[5] L. Dai, B. Wang, M. Wang, X. Yang, J. Tan, S. Bi, S. Xu, F. Yang, Z. Chen, M. Di Renzo *et al.*, "Reconfigurable intelligent surface-based wireless communications: Antenna design, prototyping, and experimental results," *IEEE access*, vol. 8, pp. 45 913–45 923, 2020.

[6] C. Huang, S. Hu, G. C. Alexandropoulos, A. Zappone, C. Yuen, R. Zhang, M. Di Renzo, and M. Debbah, "Holographic mimo surfaces for 6g wireless networks: Opportunities, challenges, and trends," *IEEE Wireless Communications*, vol. 27, no. 5, pp. 118–125, 2020.

[7] I. Yildirim, A. Uyrus, and E. Basar, "Modeling and analysis of reconfigurable intelligent surfaces for indoor and outdoor applications in future wireless networks," *IEEE transactions on communications*, vol. 69, no. 2, pp. 1290–1301, 2020.

[8] T. N. Do, G. Kaddoum, T. L. Nguyen, D. B. Da Costa, and Z. J. Haas, "Multi-RIS-aided wireless systems: Statistical characterization and performance analysis," *IEEE Transactions on Communications*, vol. 69, no. 12, pp. 8641–8658, 2021.

[9] V.-D. Phan, B. C. Nguyen, T. M. Hoang, T. N. Nguyen, P. T. Tran, B. V. Minh, and M. Voznak, "Performance of cooperative communication system with multiple reconfigurable intelligent surfaces over nakagami-m fading channels," *IEEE Access*, vol. 10, pp. 9806–9816, 2022.

[10] P. Wang, J. Fang, X. Yuan, Z. Chen, and H. Li, "Intelligent reflecting surface-assisted millimeter wave communications: Joint active and passive precoding design," *IEEE Transactions on Vehicular Technology*, vol. 69, no. 12, pp. 14 960–14 973, 2020.

[11] J. Cheng, C. Shen, Z. Chen, and N. Pappas, "Robust beamforming design for IRS-aided URLLC in D2D networks," *IEEE Transactions on Communications*, vol. 70, no. 9, pp. 6035–6049, 2022.

[12] M. Schellmann, "Capacity boosting by IRS deployment for industrial iot communication in cm-and mm-wave bands," in *2022 Joint European Conference on Networks and Communications & 6G Summit (EuCNC/6G Summit)*. IEEE, 2022, pp. 524–528.

[13] B. Zheng, C. You, and R. Zhang, "Double-IRS assisted multi-user mimo: Cooperative passive beamforming design," *IEEE Transactions on Wireless Communications*, vol. 20, no. 7, pp. 4513–4526, 2021.

[14] W. Mei and R. Zhang, "Cooperative beam routing for multi-IRS aided communication," *IEEE Wireless Communications Letters*, vol. 10, no. 2, pp. 426–430, 2020.

[15] Y. Zhang and C. You, "Multi-hop beam routing for hybrid active/passive IRS aided wireless communications," in *GLOBECOM 2022-2022 IEEE Global Communications Conference*. IEEE, 2022, pp. 3138–3143.

[16] M. Nakagami, "The m-distribution—a general formula of intensity distribution of rapid fading," in *Statistical methods in radio wave propagation*. Elsevier, 1960, pp. 3–36.